MODELING EXPERIMENTS, DESIGN AND CONSTRUCTION FOR BRIDGE SCOUR PROTECTION

Woon-Kwang Yeo
Professor, Department of Civil and Environmental Engineering, Myongji University
yeo@mju.ac.kr

Tae-In Kim
Executive Director, Geosystem Research Corp.
tikim@geosr.com

Jeong-Hwan Kim
Deputy General Manager, Samsung C&T Corporation.
jnghwan@samsung.com

Hyun-Gun Lee
General Manager, Samsung C&T Corporation
hyungun.lee@samsung.com

Byung-Sun Kim
Assistant Manager, Samsung C&T Corporation
byungsunkim@samsung.com

Dong-Wan Kim
General Manager, Samsung C&T Corporation
wallgye@samsung.com

Abstract: *The interdisciplinary and state-of-the art oceanographic investigation, numerical modeling and physical model tests to predict local scours around the piers and ship impact protections of the Incheon Grand Bridge are briefly introduced. The conceptual design and production to protect local scours are also described.*

Keywords: *Incheon Grand Bridge, local scour, oceanographic investigation, numerical modeling, physical modeling, conceptual design*

1. INTRODUCTION

When a structure is placed in a marine environment, the presence of the structure will change the flow pattern in its immediate neighborhood, causing an increase in the local sediment transport capacity and thus lead to scour. The formation of a scour hole around structure, especially bridge pier, can seriously affect the integrity of the bridge foundation, sometimes leading to failure of the bridge. In order to obtain the reasonable solution to bridge scour, an interdisciplinary co-operation has been made, in which all kinds of scour oriented researches such as oceanographic survey, scour rate test, numerical modeling, physical modeling, scour monitoring have been carried out. The flow chart of the study is presented in Fig. 1.

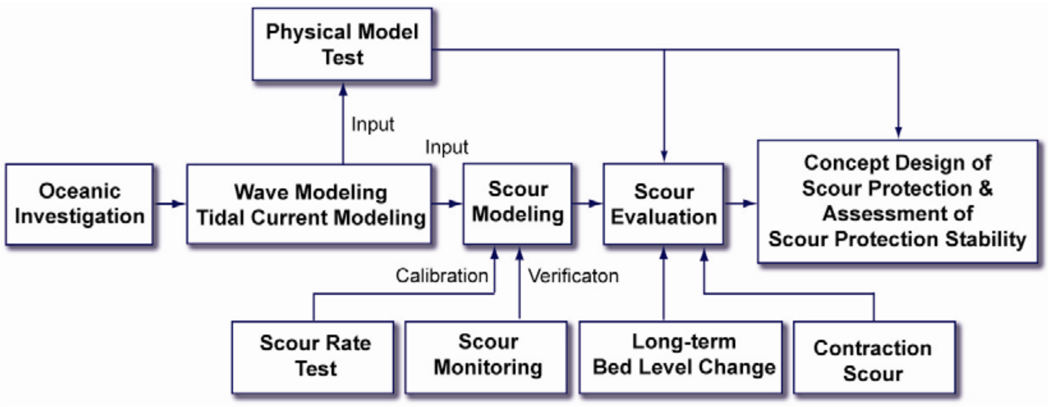

<Fig. 1> Flow chart of the study

2. OCEANOGRAPHIC INVESTIGATION

The oceanographic investigation was performed from December 2004 to January 2005 to understand the hydrodynamic and sedimentary environment around the Incheon Grand Bridges and provide input, calibration and verification data for numerical and physical modeling.
The mean sea level is 4.64 meter above the datum level (approximate lowest low water) and the estimated high water level for the return period of 100 year is 10.13 meter. The semi-diurnal and fortnightly tide characterizes the horizontal and vertical flow in the study area. The spring tidal range is 8.0 meter. The maximum current speed of 1.1 and 0.9 m/s was measured at surface and near-bottom layer, respectively near to the main pier. The southwestward ebb current is stronger by about 30% than the northeastward flood current. The bottom sediments show mixed facies of sand and mud. On average the sand comprises 63% and the mean grain size is 4φ (0.63 mm). The suspended sediment concentration was recorded to be 197 mg/L at its maximum related with high waves and strong tidal currents. The details of oceanographic investigation are described in the report [1].

3. NUMERICAL MODELING FOR LARGER DOMAIN

Numerical modeling experiments were performed to provide the design conditions such as wave and current speed for each pier and input for local bridge scour modeling, and to evaluate the hydrodymic and sedimentologic change due to the planned coastal developments nearby the bridge.
Three dimensional flow field by tide, river run-off and storm wind was simulated using the modeling system EFDC developed by Virginia Institute of Marine Sciences, the United States. The wave field generated by storm wind and swell was estimated in the modeling system SWAN developed by Delft University of Technology, the Netherlands. The design current speed and and wave height for each pier are listed in Table 1. The detailed modeling procedure and the results can also be found in the Report [1].

<Table 1> Design current speed and wave with return period of 100 year

Division	Design unit	Pier	Current speed (cm/s)		Significant wave	
			Flood	Ebb	Height (m)	Period (s)
Cable Stayed Bridge	CSB1 CSB2	W1, E1 W2-3, E2-3	120 115	149 143	2.16 2.12	5.2 5.2
Approach Bridge	ABW ABE	W4-10 E4-10	104 76	129 85	2.08 2.08	5.2 5.2
Viaduct	VW VE	W11-129 E11-59	90 62	90 58	1.95 1.82	5.2 5.2

4. NUMERICAL AND PHYSICAL MODELING FOR LOCAL SCOUR

Numerical and physical modeling experiments were carried out to estimate the extent and maximal depth of local bridge scours under extreme conditions and to provide scour protection measures around the piers and the ship impact protections. Long-termed bed level change was examined using the past nautical charts. Several empirical formulae were also applied for comparison with the numerical and physical modeling results. The overall procedure of local scour estimation is presented in Fig. 2.

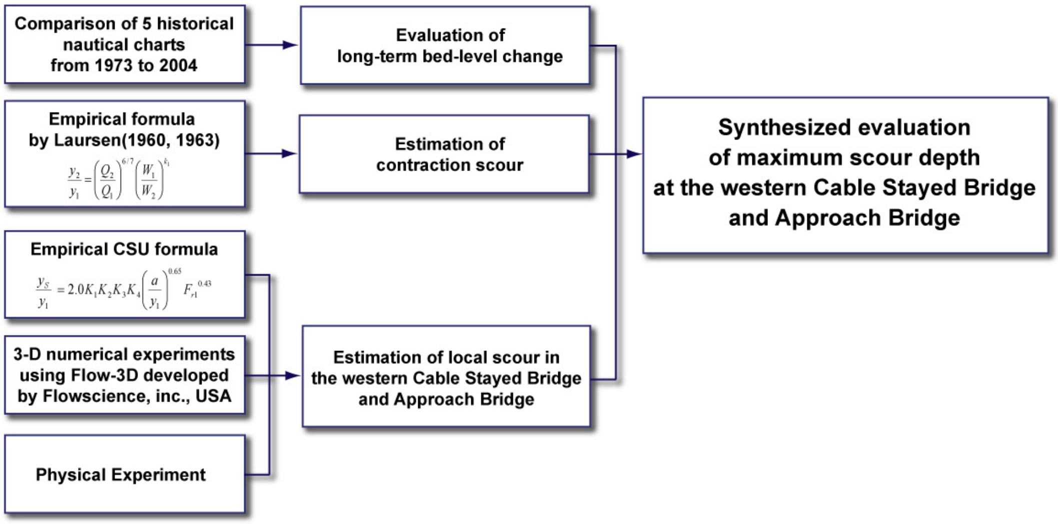

<Fig. 2> Flow chart of the local bridge scour estimation

4.1 Long-termed Bed Level Change

The historical channel cross-sections along the proposed bridge axis were analyzed to estimate the long-termed bed level change using the nautical charts No. W338 published in 1973, 1992, 1997, 2001 and 2004 by National Oceanographic Research Institute. To get a continuous depth profile along the bridge axis, the spline interpolation method was applied based on the depths acquired from the nautical charts. It is found that the bed level along the bridge axis is in equilibrium state.

4.2 Contraction Scour by Emprical Formula

Laursen's formula [2] was applied to estimate the contraction scour depth. It was calculated including the effect of the bottom sediment composition and the hydraulic condition with return period of 100 year. The contraction scour was estimated to be 0.10 meter in the western Viaduct section, 0.20 meter in the eastern Viaduct section, and 0.85 meter in the Approach and Cable-Stayed Bridge section.

4.3 Local Scour by Emprical Formula

CSU formula [3] was applied to a total of 13 piers to assess the maximum scour depth. The scour depth reaches about 19 meters in the Ship Impact Protections W1 to W4, and 10 meters in the pier W6. Scour depth calculated by the CSU formula is often overestimated, as it cannot consider cohesive and consolidated nature of bottom sediments.

4.4 Local Scour by Numerical Modeling

To reproduce three-dimensional flow structure and to estimate local scour around the piers, numerical experiments has been performed. The current and wave with return period of 100 year were applied as external forces. The model FLOW-3D is a well-known CFD program based on VOF (volume of fluid) method which was created by Los Alamos Lab in 1968 and can predict free surface, heat transfer, sediment transport and other hydraulic characteristics in three dimensions. The input parameters for scour modeling were optimized through the calibration using the results of scour rate test (Fig. 3(a)). The model was also verified using the field survey data (Fig. 3(b)). A total of 13 target piers were selected taking the pier type, water depth, bottom sediment composition, current speed and wave height into account. The maximum depth and the lateral

extent of the scour around the pier W1 is predicted to be 8.8 and 46 meter, respectively (Table 2). The distribution of surface current velocity and scour depth around the pier W1 are shown in Fig. 4.

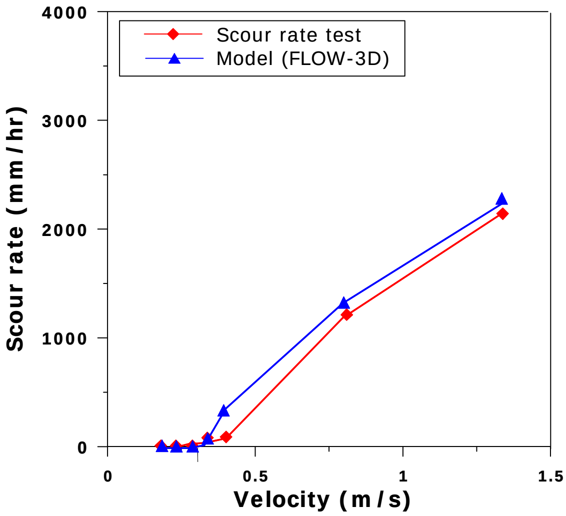

(a) Model calibration with the scour rate test (pier W9)

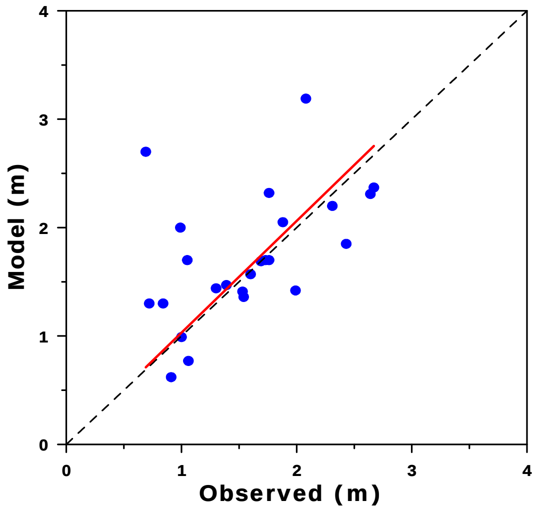

(b) Model verification with the field survey (piers W1, W4 and W11)

<Fig. 3> Model calibration and verification results

<Table 2> Maximum scour depth and extent by numerical modeling

(Unit: m)

Item	Western Viaduct					W. Approach Bridge		Cable Stayed Bridge			Eastern Viaduct		
Design unit	VW5	VW4	VW3	VW2	VW1	ABW	ABW	CSB	CSB	CSB	VE1	VE2	VE4
Pier	W80	W55	W25	W20	W11	W6	W4	W3	W2	W1	E11	E20	E47
Scour depth	2.4	3.6	4.2	4.0	4.0	5.1	7.7			8.8	2.9	2. 7	1.9
Scour extent	5	5	5	5	5	7	44			46	9	9	9

※ The critical depth for scour extent is 0.5 meter.

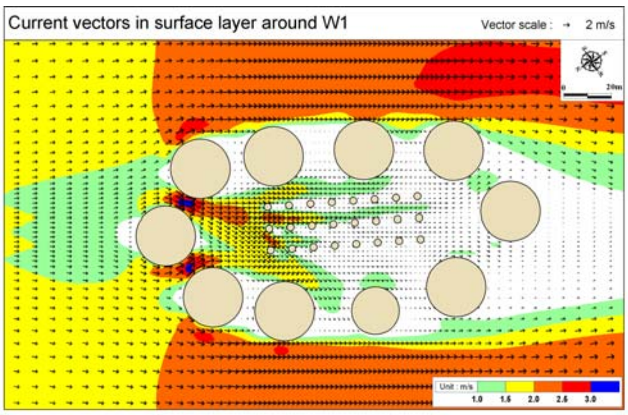

(a) Current vectors

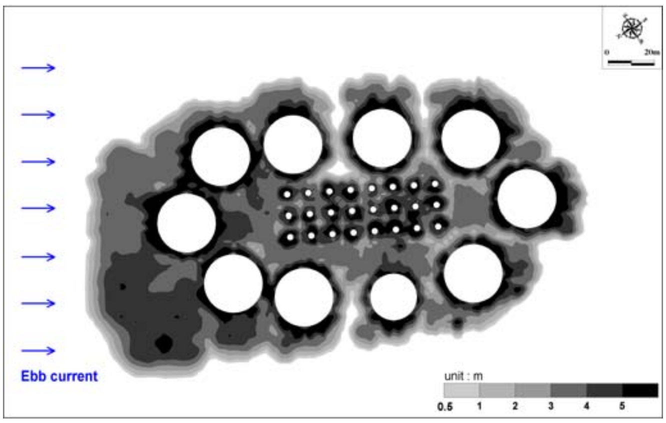

(b) Scour distribution

<Fig. 4> Numerical modeling results around the pier W1

4.5 Physical Modeling

A total of 11 piers have been tested using the physical model at a geometric scale of 1:80 to 1:36 to estimate the scour depth

and range and to confirm the stability of scour protection. Measurements from the model are reported at prototype scale by using Froude scaling. In addition to the above tests, two additional tests have been carried out under 10,000-year return period condition to verify that the proposed scour protection would satisfy the requirement of maintenance. The stability of riprap due to winnowing failure was also tested for the pier W1.

The maximum scour depth is measured to be about 5.0 m around the pier W1 (Table 3 and Fig. 5). It is found a little movement of riprap around the ship impact protections and piles at the early stage before the rocks are stabilized (Fig. 6). But the scour protections are kept stable on the whole. The movement of scour protection of W1 is less than 1% of total volume, which satisfies the criterion for design and maintenance. The experiments for riprap stability due to winnowing failure show that the ripraps are kept stable, and the sinking depths of ripraps are very small compared with the thickness of scour protection.

<Table 3> Maximum scour depth and extent by physical modeling

(Unit: m)

Item	Western Viaduct	Western Approach Bridge	Cable Stayed Bridge					Eastern Approach Bridge
Design unit	VW1	ABW	CSB					ABE
Pier	W11	W4	W3	W2	W1	E2	E3	E4
Scour depth	0.5	4.3			5.0			3.5
Scour extent	-	38			38			38

※ The critical depth for scour extent is 0.5 meter.

<Fig. 5> Physical modeling results of local scour for the pier W1

<Fig. 6> Physical modeling results of scour protection stability for the pier W1

4.6 Synthesized Evaluation

As the empirical formula cannot consider the cohesive nature of bottom sediments, its results are believed to be overestimated. The maximum scour depth and the lateral extent of scours around target piers are summarized in Table 4. The contraction

scour is not included in the maximum scour depth for the piers W1, W2, W3, W4 and W6, because the modeling domains for the piers W1 to W6 are large enough to incorporate the contraction scour. It is desirable in viewpoint of safety that the numerical and physical modeling results should be synthesized to decide the riprap extent.

<Table 4> Maximum depth and lateral extent of scours around the target piers

(Unit: m)

Method		W11	W6	W4, W3, W2	W1	E2, E3, E4	E11
Long-term bed level change		in equilibrium status					
Contraction scour		0.1	not considered as the effect of contraction is included in numerical and physical experiments				0.2
Local scour	CSU formula	2.4	9.6	19.0	19.1	-	2.2
	Numerical experiment	4.0 (5)	5.1 (7)	7.7 (44)	8.8 (46)	-	2.9 (9)
	Physical experiment	0.5	-	4.3 (37.5)	5.0 (37.5)	3.5 (37.5)	-
Total scour depth		4.1	5.1	7.7	8.8	-	3.1

※ Values in parentheses are the lateral extent of scours.

5. CONCEPTUAL DESIGN OF SCOUR PROTECTION

5.1 Design Principle of Scour Protection

If the structure is located on soil or rocky bottom, the foundation of structure should be placed below an estimated scour depth or an optimal countermeasure against scour should be established [4]. The design principles of scour protection are described in standard manuals as [5], [6], [7], [8], [9], [10] and [11].

5.2 Design Procedure of Scour Protection

In the design of scour protection, the parameters such as external forces, design unit, water depth and availability of materials are taken into account. The relevant piers are W1 to W19 and E1 to E19. The procedure of design is as follows.

5.3 Riprap Size

The riprap sizes are decided using the Isbash's formula [12]. The maximum depth-averaged current velocity with return period of 100 year in each pier obtained from the numerical experiment using FLOW-3D is applied. The armor stone size is decided by the formula of Tanimoto et al. [13, 14]. The wave height used in the calculation is the design wave height with return period of 100 year. The armor stones protect the inner riprap from wave forces. Thus the armor stones are needed if the armor stone size for the design wave is larger than the riprap size for the design current. The riprap is replaced by the armor stone if the armor stone size for the design wave is larger than the riprap size for the design current. The recommended riprap size is 50-60 cm in W1-W4 and E1-E4, and 30-40 cm in W5-W19 and E5-E19.

5.4 Range of Riprap Size

The gradation of stones in riprap affects the riprap's resistance to erosion. The stone should be reasonably well graded throughout the riprap layer thickness. Various ripraps which are larger and smaller than the recommended riprap size should be executed, and the larger ones should be placed at the upper layer for the overall stability of the scour protection. As the armor stones above lower ripraps should be in principle piled with 2 layers [5], the maximum riprap size of 70 cm can be

allowed in piers W1-W4 and E1-E4, and 50 cm in W5-W19 and E5-E19, taking the maximum riprap sizes suggested in [11] into account.

5.5 Extent of Riprap

To secure the stability of piers and ship impact protections, the lateral extent and thickness of riprap was decided by the numerical and physical modeling experiments, taking the design unit and the riprap size into account. The thickness of riprap is decided as 4Dr (riprap size) on the lateral extent of riprap taking the riprap size into account. For riprap stability, the edge slope of scour protection is decided as 18°, i.e. 1:3. The extents of riprap are listed in Table 5. The plan view of the scour protection is shown in Fig. 7.

<Table 5> The extent of scour protection

Classification	Relevant piers	Lateral extent (m)		Thickness (m)
		Top	Bottom	
West	W1 - W4 W5 W6 - W19	37.5 (=1.5 BSIP) 10 (≒4 BP) 10 (≒6 BP)	45.0 (=1.8 BSIP) 14.5 (≒6 BP) 14.5 (≒8 BP)	2.5 (≒4 Dr) 1.5 (≒4 Dr) 〃
East	E1 - E4 E5 - E8 E9 - E19	37.5 (=1.5 BSIP) 10 (≒4 BP) 10 (≒6 BP)	45.0 (=1.8 BSIP) 14.5 (≒6 BP) 14.5 (≒8 BP)	2.5 (≒4 Dr) 1.5 (≒4 Dr) 〃

※ BSIP (=25 m) is the diameter of the ship impact protection.
※ BP is the diameter of the pier, which is 2.4 and 1.8 m for W5 (E5) and W6 to W19 (E6 to E19), respectively.
※ Dr is the riprap size, which is 55 and 35 cm for W1 - W4 (E1 - E4) and W5 - W19 (E5 - E19), respectively.

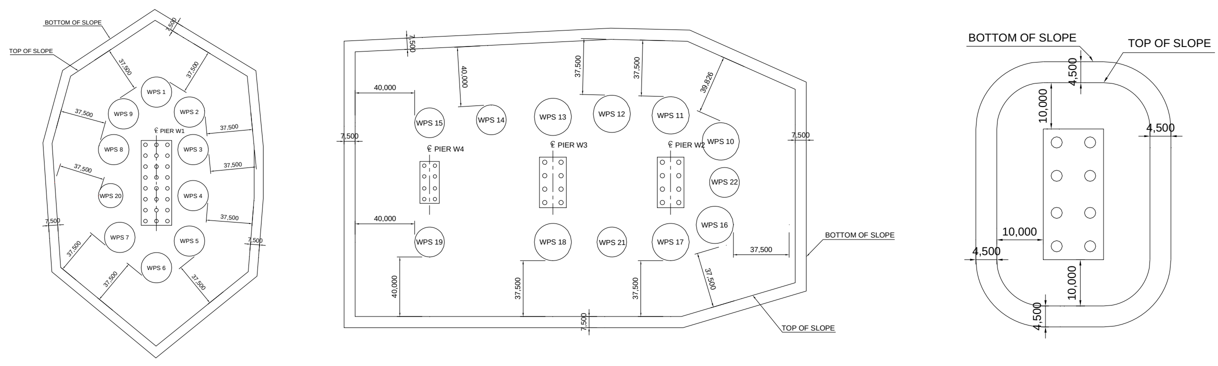

(a) W1 (b) W2-W4 (c) W5-W19 (E5-E19)

<Fig. 7> Plan views of scour protection

5.6 Filter Layers

The ripraps sinking by bottom sediment escaping (winnowing failure) was estimated by physical experiment for scour protection. According to the results of physical experiments for W1, the ripraps are kept stable, and the sinking depths of ripraps are very small compared with the thickness of scour protection. Therefore there may be no problem in stability of the ripraps, even if the filter layers are not executed.

5.7 Rock Gabions

The stability of riprap was estimated by physical experiment for scour protection. According to the results of physical experiments, some ripraps were scattered a little, but riprap protection kept stable on the whole. The amount of riprap scattered is within the criterion for design and maintenance. Therefore there may be no problem in stability of the riprap protection, even if rock gabion is not executed.

6. CONSTRUCTION OF SCOUR PROTECTION

6.1 Construction Sections

The sections in which scour protection is constructed are the cable-stayed bridge (W(E)1~4), approach bridges (W(E)5~10) and viaduct (W(E)11~19) of Incheon Bridge shown in Fig. 8.

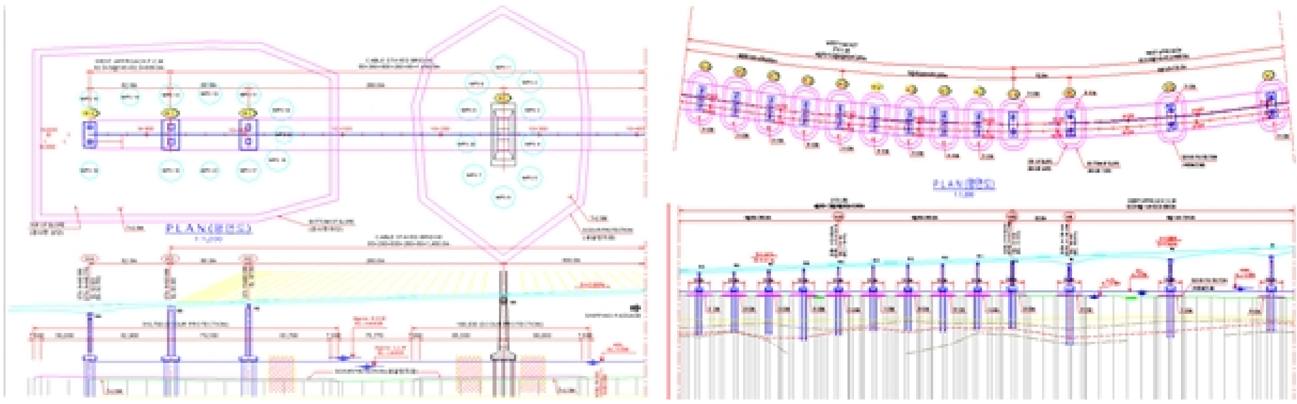

(a) Cable-stayed bridge (b) Approach bridges and viaduct

<Fig. 8> Scour protection of Incheon Bridge

6.2 Construction Details (Fig. 9)

<u>**Cable-Stayed Bridge Section (W(E)1~4)**</u>

Laying range of scour protection: 37.5 m
Laying height of scour protection: 2.5 m
- Lower section H = 1.2 m (dimensions of riprap: smaller than 500 mm)
- Upper section H = 1.3 m (dimensions of riprap: 500~700 mm)

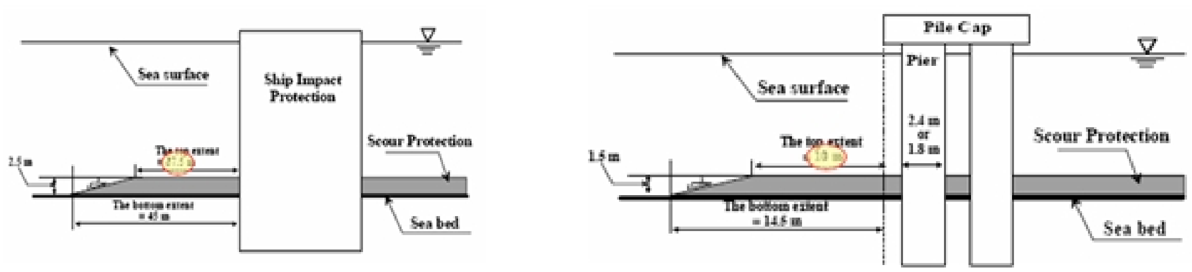

(a) Cable-stayed bridge (b) Approach bridges and viaduct

<Fig. 9> Cross-sections of scour protection

<u>**Approach Bridges and Viaduct Sections (W(E)5~19)**</u>

Laying range of scour protection: 10.0 m
Laying height of scour protection: 1.5 m
- Lower section H = 0.7 m (dimensions of riprap: smaller than 300 mm)
- Upper section H = 0.8 m (dimensions of riprap: 300~500 mm)

6.3 Equipment for Scour Protection Construction

<u>**Production and Loading of Riprap**</u>

Back hoe: Loading of riprap
Breaker: Crushing of riprap
Drill: Boring of holes for charging with explosives
Loader: Transport of riprap
Crusher: Crushing of riprap to specified dimensions
Dump truck: Transport of riprap / Loading of riprap on ship

Transport and Dropping of Riprap

Back hoe: Dropping of riprap
S. Barge: Setting of dropping zone during dropping of riprap
F. Barge: Loading of riprap
Conveyer: Dropping near cells and piles
Diving equipment: Installation of buoy / Check of levelling
Tugboat: Pulling and setting of riprap barge
Electric generator: Night time lighting and supply of electric power

6.4 Construction Conditions

The conditions during the construction of the scour protection were as follows:

- Wind speed < 10 m/s
- Tide < 5.0 knot
- Visibility > 1.0 km
- Tide < 10 m/s

Flowchart of the production and transport of riprap and that of dropping are presented in Figs. 10 and 11, respectively.

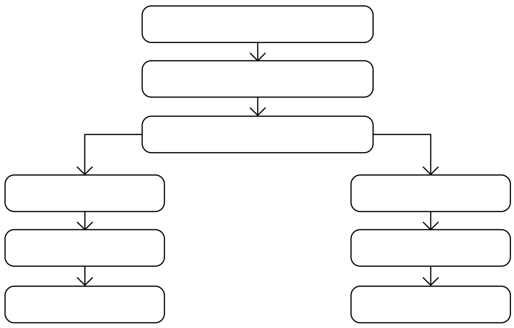

<Fig. 10> Flowchart of production and transport of riprap

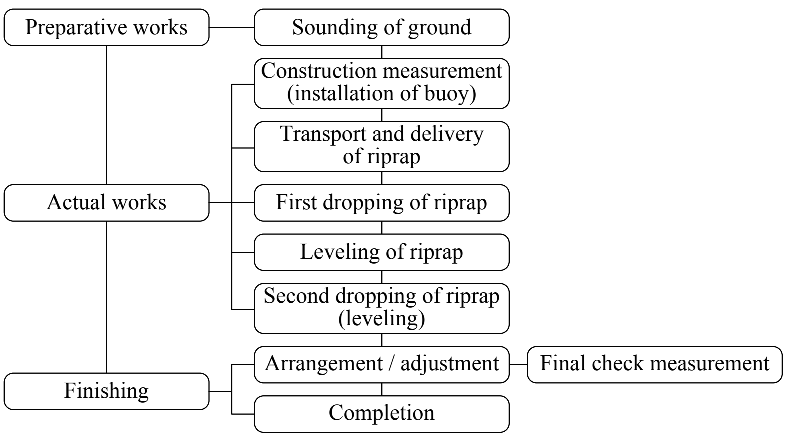

<Fig. 11> Flowchart of on-site dropping of riprap

6.5 Construction Cycle

The position of loading of riprap located at Sammok 2 Island is distant by about 34 km from the site. Therefore, the computation of the transport cycle time gives the following:

- For barge 3000~5000P, loading time: 4 hours
- For transportation speed of 7.2 km, transport time: about 5 hours
- For sail round speed of 7.2 km/hr, navigation time: about 4 hours
- Dropping time: 6 hours on the mean
- Other (loading stand-by, dropping stand-by, etc.): 5 hours

Accordingly, one transport cycle was calculated as 24 hours. The water depth being very low between Mueui Island and Youngjong Island, navigation was conducted considering the time schedule. Moreover, the cycle time was calculated by estimating the tide because of different transport time according to neap tide and ebb tide.

6.6 Dropping Method of Riprap

Preliminary Ground Sounding

The S. barge is disposed by means of electro-optical measurement at the preliminary assigned location on the ballast of the installed lot. The seabed ground altitude is measured and check is received from the supervisor. The S. barge is then set. Thereafter, the eventual difference between the measured ground depth and the design values is verified using a depth sounder and dispatching divers. Places presenting large difference with the design values or steep slope are indicated by buoy to mark spots requiring special management during dropping.

Marking Method of Riprap Dropping Places (Installation of Buoy)

At the approach bridges and viaduct sections, the F. barge is brought alongside the S. barge and the S. barge is moved to the riprap dropping position using a distance estimator. At the cable-stayed bridge section, an electro-optical measurement device is adopted to appoint the dropping position since setting is extremely delicate through the use of the distance estimator only, and the buoys are installed after hanging weights. The color of the flags is red and the flags were also installed to protect the working site and prevent safety accident with the navigating ships. Tapeline and electro-optical measuring devices were used to find the exact position during the installation. Measurement was conducted by installing the electro-optical device on the foundation and the prism in the S. barge. The coordinate set-out measurement was performed in the absence of tide to be free from the effects of the tides and waves.

Riprap Dropping at the Viaduct and Approach Bridges

The setting of the F. barge was impossible in the western approach bridge due to the tide. Such situation lengthened the stand-by time of the barges. Since the construction surface was exposed at low tides, the riprap was dropped at once during high tides and levelling was executed through B/H (1.0 m^3, 0.2 m^3) by launching a footboard from the barge.
Since work was conducted once the construction surface was exposed at low tide, the available working days reached merely 6 to 7 days per month. Therefore, a thorough schedule for the utilization of the equipment was of crucial importance. In addition, the design predicted a width of 10 m between the foundation and the dropping position at the viaduct section. However, only a smaller width of 7 m was available when the S. barge and F. barge were standing alongside. Accordingly, the design quantities were dropped at once in the space of 7 m at the western side and levelling was executed by unloading the B/H. At the eastern side, the 7 m space was constructed in advance and riprap was then dropped in the remaining 3 m space by moving the S. barge, which loaded and transported the riprap independently (Fig. 12).
In the eastern approach bridge, dropping was performed without spatial limitation. However, a specially fabricated tremie pipe was installed to perform riprap dropping up to the bottom of the foundations at the bottom of the foundations and around the piles (Fig. 13).

<Fig. 12> Independent operation of setting barge

<Fig. 13> Dropping through tremie pipe

Riprap Dropping at the Cable-Stayed Bridge

The cable-stayed bridge section is characterized by rapid currents and frequent passage of passenger liners and ocean liners, which make it frequently exposed to cruising waves in addition to the interference of the anchors with the navigation channel. Accordingly, construction was carried out by checking and managing the weather conditions and the navigation logs of the liners. The construction area at the cable-stayed bridge being very wide, dropping was executed by dividing the area in several lots as shown in Fig. 14. Works were always done by moving the S. barge.
Twenty-meter long measurement rods were installed on the cells of the ship collision protection. These rods were used to evaluate the EL. Values after measurement of the water level according to time so as to manage the dropping of riprap. Moreover, the sections where ship collision protection was not installed were identified and dropping was forbidden in these sections. Construction was executed to avoid hindrance to pile driving.

Generals of Riprap Dropping

Since the riprap was dropped from the surface of the water and could be laid to another position due to the tidal effect during the first dropping, dropping was executed with sufficient consideration of the tide. Work was performed as possible at low tide to minimize the tidal effects. After completion of the first dropping, the overall status was measured by means of a depth sounder over a definite section and the dropping results were estimated using the measured values to provide reference for the second dropping and enable more exact works.

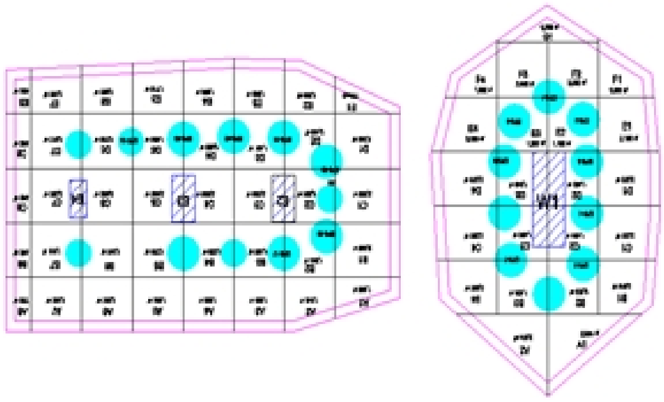

<Fig. 14> Section allotment at the cable-stayed bridge

Levelling of Riprap

The levelling at the western approach bridge and viaduct sections was carried out directly through B/H. However, the final levelling at the eastern approach bridge, viaduct and cable-stayed bridge sections was executed through close and precise dropping by dispatching divers before and after riprap dropping. Levelling works were subdivided into two stages. The first stage levelling was performed after dropping of sized riprap with dimensions below 300 mm at the approach bridges and viaduct and below 500 mm at the cable-stayed bridge. The second stage levelling was executed to obtain the final designed height by dropping sized riprap with dimensions of 300~500 mm at the approach bridges and viaduct and 500~700 mm at the cable-stayed bridge.
Since dropping was executed 24 hours per day, the levelling of riprap was implemented immediately after completion of 1 riprap dropping cycle by the S. barge. The portions with height lower than the planned level were detected by divers who checked the quantities. The exact positions of the defective portions were evaluated after communication with the surface and adjusted through precise dropping by B/H. The divers being performing underwater works, team work among the divers, assistants and equipment is of extreme importance. Particular attention should be paid to safety accidents since transport and dropping are done in submarine environment with poor visibility.

Setting of Barges

The western approach bridge and viaduct sections being significantly influenced by the tide level, the barges should be set at high tide considering the periods of tide level. The current speed is extremely high during the highest tide, which renders the fixation of the anchors and travelling of the barges difficult. Accordingly, works were executed at periods with the lowest tidal changes. The setting of the barges at the viaduct was done in an X-shape with the barge at the center between the piers due to the narrow space between the piers. Construction was conducted on both sides at the right and left side piers. In the case of the approach bridge, the large space between the piers exceeded the working radius of the back hoe and required 2 settings for dropping.
For the cable-stayed bridge, a conveyer barge was used for dropping at the inner side of the ship collision protection cells and around the piles. Outside the cells, the back hoe was adopted for dropping using the S. barge. In the portions of the cable-stayed bridge interfering with the ship collision protection structure, the barge was fixed by the 11-shape setting method or using soft ropes attached to the cell structures in the case where the anchors could not be rooted by the X-shape method. For the main navigation channel, risk of winding with the screw of the barges may occur when the strip of the anchor buoy engages in the navigation channel. Therefore, the anchors were thrown after removal of the buoys and the anchors were removed by pulling the rope using the winch of the tugboat.

Construction Conditions and Methods according to Tide

When the tidal difference of the daily flux and reflux is small, the transport of the riprap becomes easier since the flow of the surface water is stabilized. At that time, the riprap levelling and dropping were executed simultaneously enabling to perform the dropping works within 9 to 10 hours. When the tidal difference is the largest, the seawater rises together with the instability of the surface water flow. Considering that, in such conditions, the simultaneous execution of the levelling and dropping of riprap become difficult, the setting of the barge was performed once again after temporary works of about 4 to 5 hours.

7. CONCLUDING REMARKS

To estimate the local scour depth and extent exactly, state-of-the-art numerical and physical modeling techniques have been applied to the Incheon Grand Bridge based on the intensive oceanogrphic investigation. The scour depth and extent estimated by numerical modeling are rather larger than those by physical modeling. The riprap sizes were decided by the formula of Isbash and Tanimoto et al. The recommended riprap size is 0.5 to 0.6 meter for the piers W1 to W4 and E1 to E4, and is 0.3 to 0.4 meter for the piers W5 to W19 and E5 to E19. The lateral boundary of riprap is recommended to be 45 meter for the piers W1 to W4 and E1 to E4, and 14.5 m for the piers W5 to W19 and E5 to E19. Physical model tests showed that the top ripraps of scour protection were scattered a little i.e. less than 1% of total volume of scour protection at the pier W1. The scour protection of the pier W10 remained stable. These results satisfy the criteria for 10,000-year return period event. Nevertheless periodic monitoring and inspection are necessary to detect any probable scour or failure of scour prevention measures.

REFERENCES

[1] Samsung Corporation JV, 2005, Oceanographic Investigation Report, Design Package No. 2, Incheon 2nd Bridge Project, Document No. DSN-02-S&I-OIR(E), 716p.

[2] E. Laursen, 1963, "An analysis of relief bridge scour," Journal Hydraulic Division, American Society of Civil Engineers, 89, HY3.

[3] E. Richardson, D. Simons, S. Karaki, K. Mahmood and A. Stevens, 1975, Highways in the River Environment, Hydraulic and Environmental Design Considerations Training and Design Manual, FHWA.

[4] Ministry of Construction & Transportation, 2005a, Standard for Design of the Highway Bridge, Korea Road & Transportation Association, 380p.

[5] Ministry of Maritime Affairs & Fisheries, 2005, The Standard for Port and Harbor Design, 1637p.

[6] Ministry of Construction Transportation, 2005b, Standard for Design of the Road, Korea Road & Transportation Association, 510p.

[7] Ministry of Construction & Transportation, 2002, Standard for Design of Riverine Construction, Korea Water Resources Association, 861p.

[8] U.S. Army Coastal Engineering Research Center, 2001, Shore Protection Manual, II.

[9] U.S. Department of Transportation Federal Highway, 1989, Hydraulic Engineering Circular-11(HEC-11), Design of Riprap Revetment.

[10] U.S. Department of Transportation Federal Highway, 2001, Hydraulic Engineering Circular-23 (HEC-23), Bridge Scour and Stream Instability Countermeasures (Experience, Selection, and Design Guidance Second Edition).

[11] American Association of State Highway and Transportation Officials, 1999, Model Drainage Manual, Metric Edition.

[12] S. Isbash, 1936, "Construction of dams by depositing rock in running water," Transactions, Second Congress on Large Dams, Washington, D.C., U.S.A., 126-136.

[13] K. Tanimoto, et al., 1982a, Stability of armour units for foundation mounds of composite breakwaters by irregular wave tests, Rept. Port and Harbour Res. Inst., 21, 3, 3-42 (in Japanese).

[14] K. Tanimoto, T. Yagyu, and Y. Goda, Y., 1982b, "Irregular wave tests for composite breakwater foundations," Proc. 18th Int. Conf. Coastal Eng., Cape Town, 2144-2163.